

NFN - Nationales Forschungsnetzwerk

Geometry + Simulation

<http://www.gs.jku.at>



---

**Bases and dimensions of  
 $C^1$ -smooth isogeometric  
splines on volumetric  
two-patch domains**

Katharina Birner and Bert Jüttler  
and Angelos Mantzaflaris

G+S Report No. 61

November 2017

---

**FWF**

Der Wissenschaftsfonds.

**JKU**  
JOHANNES KEPLER  
UNIVERSITY LINZ

# Bases and dimensions of $C^1$ -smooth isogeometric splines on volumetric two-patch domains

Katharina Birner<sup>a,\*</sup>, Bert Jüttler<sup>a</sup>, Angelos Mantzaflaris<sup>a</sup>

<sup>a</sup> Institute of Applied Geometry, Johannes Kepler University Linz, Austria

## Abstract

We analyze the spaces of  $C^1$ -smooth isogeometric functions on hexahedral two-patch domains. Our aim is to generalize the corresponding results from the bivariate [25] to the trivariate case. In the first part of the paper, we introduce the notion of gluing data and use it to define glued spline functions on two-patch domains. Employing the fundamental observation that “matched  $G^k$ -constructions always yield  $C^k$ -continuous isogeometric elements” [14], this allows us to characterize  $C^1$ -smooth geometrically continuous isogeometric functions as the push forwards of these functions for suitable gluing data. The second part of the paper is devoted to various special classes of gluing data. We analyze how the generic dimensions depend on the number of knot spans (elements) and on the spline degree. Finally we show how to construct locally supported basis functions in specific situations.

*Keywords:* geometric continuity, isogeometric analysis, volumetric multi-patch domain,  $C^1$ -smooth isogeometric functions

## 1 Introduction

One of the main advantages of the framework of isogeometric analysis (IGA) [3, 9], which was established by T.J.R. Hughes et al in 2005 [18], is that it allows for discretization spaces providing high order smoothness. Using these spaces can be beneficial when solving high order partial differential equations, such as the Cahn-Hilliard equation [10, 12], the Navier-Stokes-Korteweg equation [13] as well as Kirchhoff-Love shells [2, 4, 26].

More precisely, the use of tensor-product splines – which dominate in applications due to their frequent use in Computer-Aided Design – lead to isogeometric discretization spaces that possess high order smoothness within each patch. However, multi-patch parameterizations are required when considering more complex geometries, and the construction of globally smooth spline functions is a non-trivial problem. This has motivated research on the coupling of isogeometric multi-patch spline spaces across interfaces. Two main approaches can be identified:

On the one hand, the coupling constraints are enforced weakly, using variational methods or Lagrangian multiplier-based techniques. Nitsche-type methods in IGA were studied in [1, 30], and the particular case of isogeometric thin shells were considered in [15]. Isogeometric mortar methods have been investigated in [6], whereas discontinuous Galerkin methods were

---

\*Corresponding author (katharina.birner@jku.at)

explored in [27]. More recently, the latter approach has been extended to provide isogeometric tearing and interconnecting solvers [16].

On the other hand, the coupling constraints are enforced strongly, by defining a suitable subset of the isogeometric spline space on the underlying multi-patch domain. We will follow this approach in our paper.

The strong enforcement of the coupling constraints is particularly well suited for generating  $C^0$ -smooth isogeometric splines on multi-patch domains. In [32] isogeometric spline forests were introduced and the potential to use them as a basis in the isogeometric context was shown. Multi-patch B-splines with enhanced smoothness across the interface were described in [7].

The construction of isogeometric discretizations possessing higher order smoothness is a more involved problem. Most methods use the concept of geometric continuity [31] and the fundamental observation that  $C^s$ -continuity of an isogeometric function is directly related to  $G^s$ -smoothness (order  $s$  geometric continuity) of the associated parameterization [14]. With a few exceptions, the majority of the literature on (at least)  $C^1$ -smooth isogeometric multi-patch splines addresses the bivariate case.

A detailed investigation of  $C^1$ -smooth piecewise polynomial splines on bilinearly parameterized multi-patch domains has been given by [5]. General results on dimensions and bases of geometrically continuous spline surfaces of arbitrary topology were presented recently [28]. The space of  $C^1$ -smooth geometrically continuous isogeometric splines on bilinear two- and multi-patch domains was studied in [19, 25], including explicit constructions of basis functions and numerical experiments indicating optimal approximation power. Recently, these results have been extended to  $C^2$ -smoothness [22, 23, 24].

The notion of analysis-suitable  $G^1$ -parameterizations, which was introduced in [8], generalizes the piecewise bilinear case while maintaining the optimal approximation properties. The detailed analysis for two- and multi-patch domains is provided in [21] and [20], respectively.

To the best of our knowledge, the only existing construction of  $G^1$ -smooth isogeometric splines in the trivariate case was presented by [29]. It was derived by applying a sweep operation to a bivariate construction, hence the effect of geometric continuity is limited to two of the three parametric directions.

The present paper extends the investigation of  $G^1$ -smooth isogeometric splines on two patch domains (cf. [25]) to the volumetric setting.

In the first part of the paper, which consists of Sections 2 and 3, we introduce the notion of gluing data and use it to define glued spline functions on two-patch domains. Employing the fact that “matched  $G^k$ -constructions always yield  $C^k$ -continuous isogeometric elements” [14], this allows us to characterize  $C^1$ -smooth geometrically continuous isogeometric functions as the push forwards of these functions for suitable gluing data. The second part of the paper (Sections 4–6) is devoted to various special classes of gluing data. We analyze how the generic dimensions depend on the number of knot spans (elements) and on the spline degree. We also show how to construct locally supported basis functions in specific situations. We conclude the paper in Section 7.

## 2 Glued spline spaces

We restrict ourselves to a two-patch domain  $\Omega = \Omega^{(1)} \cup \Omega^{(2)}$ , which consists of two hexahedral volumetric subdomains  $\Omega^{(1)}$  and  $\Omega^{(2)}$  that share a common face. Both subdomains

are described by parameterizations  $\mathbf{F}^{(i)} : [0, 1]^3 \rightarrow \Omega_i$ , see Fig. 1. In particular, we consider parameterizations by spline functions.

Let the symbol  $\mathcal{S}_{s,k}^p$  denote the space of spline functions on  $[0, 1]$  of degree  $p$  with  $k$  uniformly distributed inner knots of multiplicity  $p - s$ . Consequently, this space contains spline functions that are at least  $C^s$  smooth. The two hexahedral subdomains are described by parametric representations  $\mathbf{F}^{(1)}$  and  $\mathbf{F}^{(2)}$  with coordinate functions from the tensor-product spline space

$$\mathcal{P} = \mathcal{S}_{1,k}^p \otimes \mathcal{S}_{1,k}^p \otimes \mathcal{S}_{1,k}^p,$$

for certain values of the degree  $p$  and the knot number  $k$ . These parameterizations, which are defined on two copies of the domain  $[0, 1]^3$ , form the *two-patch geometry mapping*

$$\mathbf{F} = (\mathbf{F}^{(1)}, \mathbf{F}^{(2)}) \in \mathcal{P}^3 \times \mathcal{P}^3.$$

We assume that the common face of the subdomains is parameterized by the two copies of the face  $\Gamma = [0, 1]^2 \times \{0\}$  of the domains. More precisely, the subdomain parameterizations satisfy

$$\mathbf{F}^{(1)}(\xi_1, \xi_2, 0) = \mathbf{F}^{(2)}(\xi_1, \xi_2, 0). \quad (1)$$

*Isogeometric discretization spaces* on the two-patch domain  $\Omega$ ,

$$(\mathcal{P} \times \mathcal{P}) \circ \mathbf{F}^{-1},$$

are constructed by composing pairs of spline functions belonging to  $\mathcal{P} \times \mathcal{P}$  with the inverse of the geometry mapping  $\mathbf{F}$ . Additional constraints are needed to construct smooth isogeometric discretizations. More precisely, we will use gluing data to identify a suitable subspace of the full Cartesian product  $\mathcal{P} \times \mathcal{P}$ . Both the two-patch geometry mapping and the functions used for the discretizations will be chosen from the *glued spline space*, which is defined in the following:

We denote by  $\Pi$  the ring of polynomials in two variables. Additionally, let  $\Pi_*$  be the ring of bivariate piecewise polynomial functions on  $[0, 1]^2$ , which are obtained by composing finitely many polynomial segments of arbitrary degree. In the most general case, the gluing data

$$D = (\alpha_1, \alpha_2, \alpha_3, \alpha_4) \in \Pi_*^4$$

is a quadruple consisting of four bivariate piecewise polynomials  $\alpha_i$ ,  $i = 1, \dots, 4$ .

We say that gluing data  $D$  is *regular*, if both  $\alpha_3$  and  $\alpha_4$  are *non-zero*, i.e., these functions satisfy the inequality

$$\alpha_3(s, t) \cdot \alpha_4(s, t) \neq 0 \quad \forall (s, t) \in [0, 1]^2.$$

Given some gluing data  $D$ , which may or may not be regular, we define the *glued spline space*

$$\mathcal{G}_D = \left\{ \mathbf{f} = (f^{(1)}, f^{(2)}) \in \mathcal{P}^2 : \underbrace{f^{(1)} = f^{(2)} \text{ on } \Gamma}_{(a)} \text{ and } \underbrace{\alpha_1 \partial_1 f^{(1)} - \alpha_2 \partial_2 f^{(1)} + \alpha_3 \partial_3 f^{(1)} - \alpha_4 \partial_3 f^{(2)} = 0 \text{ on } \Gamma}_{(b)} \right\},$$

which is the subspace of the Cartesian product  $\mathcal{P} \times \mathcal{P}$  consisting of pairs of functions that satisfy the continuity condition (a), which involves the values of both functions on the interface, and the additional derivative compatibility condition (b). The partial derivative operator  $\partial_k$  indicates the differentiation with respect to the  $k$ -th argument  $\xi_k$ .

We briefly discuss two special cases:

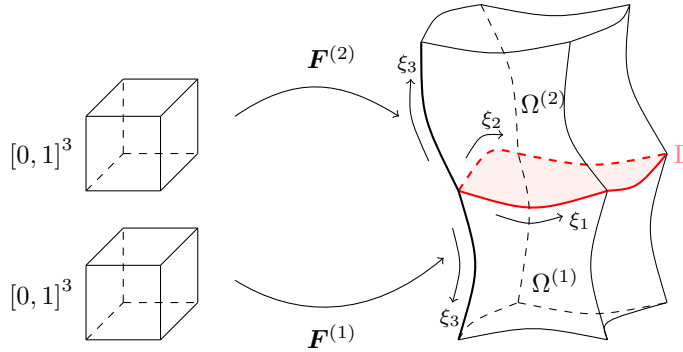


Figure 1: Parameterizations of two hexahedral subdomains  $\Omega^{(1)}$  and  $\Omega^{(2)}$  with the same parameter domain, joined at the interface  $\Gamma$ .

- When choosing trivial data  $D_0 = (0, 0, 0, 0) = \mathbf{0}$ , the compatibility condition is satisfied for any choice of the two functions, hence we obtain the space  $\mathcal{G}_0$  consisting of pairs of spline functions that are joined together with  $C^0$ -smoothness. This space contains any space defined by non-trivial gluing data  $D$ .
- We obtain pairs of spline functions with identical first derivatives along the interface when choosing  $D_1 = (0, 0, 1, 1)$ . This corresponds to the classical case of spline functions that are joined together with  $C^1$ -smoothness.

In the sequel we will use the B-spline representation

$$f^{(i)} = \sum_{k=0}^n b_k^{(i)} N_k(\xi_1, \xi_2, \xi_3), \quad i \in \{1, 2\},$$

of the functions  $\mathbf{f} = (f^{(1)}, f^{(2)}) \in \mathcal{P} \times \mathcal{P}$ , where  $N_k$  are the tensor-product B-splines spanning the space  $\mathcal{P}$ . Consequently, any function  $\mathbf{f} \in \mathcal{G}_D$  is characterized by the two equations

$$\begin{aligned} 0 &= \sum_{k=0}^n b_k^{(1)} N_k(\xi_1, \xi_2, 0) - b_k^{(2)} N_k(\xi_1, \xi_2, 0) \quad \text{and} \\ 0 &= \sum_{k=0}^n b_k^{(1)} \left( \alpha_1(\xi_1, \xi_2) (\partial_1 N_k)(\xi_1, \xi_2, 0) - \alpha_2(\xi_1, \xi_2) (\partial_2 N_k)(\xi_1, \xi_2, 0) \right. \\ &\quad \left. + \alpha_3(\xi_1, \xi_2) (\partial_3 N_k)(\xi_1, \xi_2, 0) \right) - b_k^{(2)} \alpha_4(\xi_1, \xi_2) (\partial_3 N_k)(\xi_1, \xi_2, 0). \end{aligned} \quad (2)$$

The next section discusses the relation between glued spline spaces and smooth isogeometric discretizations. This is then followed by an analysis (presented in Section 4) of the dimension of the glued spline space  $\mathcal{G}_D$  for various different choices of gluing data  $D$ .

### 3 Geometrically continuous isogeometric functions

We consider geometry mappings  $\mathbf{F} \in \mathcal{G}_0^3$ , hence the  $C^0$  condition (1) is satisfied. For each mapping  $\mathbf{F}$  we define the space

$$\mathcal{V}_{\mathbf{F}} = [(\mathcal{P} \times \mathcal{P}) \circ \mathbf{F}^{-1}] \cap C^1(\Omega^{(1)} \cup \Omega^{(2)})$$

of  $C^1$ -smooth isogeometric functions on the computational domain  $\Omega$ .

In detail, we consider functions  $\nu \in (\mathcal{P} \times \mathcal{P}) \circ \mathbf{F}^{-1}$ . For any such function  $\nu$  there exist two spline functions  $w^{(1)}, w^{(2)} \in \mathcal{P}$  such that

$$(\nu|_{\Omega^{(i)}})(\mathbf{x}) = \nu^{(i)}(\mathbf{x}) = (w^{(i)} \circ (\mathbf{F}^{(i)})^{-1})(\mathbf{x}), \quad \mathbf{x} \in \Omega^{(i)}, \quad i = 1, 2.$$

or equivalently

$$(\nu|_{\Omega^{(i)}})(\mathbf{F}^{(i)}(\boldsymbol{\xi})) = \nu^{(i)}(\mathbf{F}^{(i)}(\boldsymbol{\xi})) = w^{(i)}(\boldsymbol{\xi}), \quad \boldsymbol{\xi} \in [0, 1]^3, \quad i = 1, 2.$$

As additional smoothness property we require that the first derivatives of  $\nu^{(1)}$  and  $\nu^{(2)}$  take identical values at the interface  $\mathbf{F}^{(i)}(\xi_1, \xi_2, 0)$ ,  $i \in \{1, 2\}$ , since  $\nu \in C^1(\Omega^{(1)} \cup \Omega^{(2)})$ .

We consider the associated *graph surface*  $\Phi$  of  $\nu$ , which consists of two patches

$$\Phi^{(i)} = \left( \mathbf{F}^{(i)}, w^{(i)} \right)^T : [0, 1]^3 \rightarrow \mathbb{R}^4, \quad i = 1, 2.$$

The function  $\nu$  is  $C^1$ -smooth if and only if the two patches have identical tangent hyperplanes along the interface

$$\Phi^{(1)}(\xi_1, \xi_2, 0) = \Phi^{(2)}(\xi_1, \xi_2, 0), \quad \xi_1, \xi_2 \in [0, 1], \quad (3)$$

see Theorem 1 in [25] for the bivariate case. This is characterized by two conditions: First, the spline functions  $w^{(i)}$  satisfy the  $C^0$  condition

$$w^{(1)}(\xi_1, \xi_2, 0) = w^{(2)}(\xi_1, \xi_2, 0).$$

Second, the four partial derivatives

$$\begin{aligned} \partial_1 \Phi^{(1)}(\xi_1, \xi_2, 0) &= \partial_1 \Phi^{(2)}(\xi_1, \xi_2, 0), \\ \partial_2 \Phi^{(1)}(\xi_1, \xi_2, 0) &= \partial_2 \Phi^{(2)}(\xi_1, \xi_2, 0), \\ \partial_3 \Phi^{(1)}(\xi_1, \xi_2, 0) &\text{ and } \partial_3 \Phi^{(2)}(\xi_1, \xi_2, 0) \end{aligned} \quad (4)$$

of both patches are linearly dependent at each point of the interface (3). These conditions are equivalent to the well-established notion of geometric continuity between patches (see [14, 17]), hence we refer to  $\mathcal{V}_{\mathbf{F}}$  as the space of  $C^1$ -smooth geometrically continuous isogeometric functions.

The linear dependency can be equivalently characterized by the vanishing determinant of the  $4 \times 4$  matrix consisting of the vectors in (4). The resulting equation

$$J(\xi_1, \xi_2) = \det \begin{pmatrix} \nabla \mathbf{F}^{(1)}|_{\xi_3=0} & \partial_3 \mathbf{F}^{(2)}|_{\xi_3=0} \\ \nabla w^{(1)}|_{\xi_3=0} & \partial_3 w^{(2)}|_{\xi_3=0} \end{pmatrix} = 0 \quad (5)$$

generalizes the well-known determinant condition for geometric continuity of surfaces [17]. We consider the expansion of this determinant by its first minors  $J_{4m}$  and obtain

$$J_{41} (\partial_1 w^{(1)}|_{\xi_3=0}) - J_{42} (\partial_2 w^{(1)}|_{\xi_3=0}) + J_{43} (\partial_3 w^{(1)}|_{\xi_3=0}) - J_{44} (\partial_3 w^{(2)}|_{\xi_3=0}) = 0.$$

For future reference we note that

$$J_{44} = \det \nabla \mathbf{F}^{(1)}|_{\xi_3=0} \quad \text{and} \quad J_{43} = \det \nabla \mathbf{F}^{(2)}|_{\xi_3=0}.$$

These minors define the *geometric gluing data*

$$D_{\mathbf{F}} = (J_{41}, J_{42}, J_{43}, J_{44}). \quad (6)$$

We call it geometric as it is obtained from a geometry mapping  $\mathbf{F}$ .

Two observations are in order:

- The coordinate functions of the two-patch geometry mapping  $\mathbf{F}$  are elements of the glued spline space defined by the geometric gluing data  $D_{\mathbf{F}}$ , i.e.,

$$\mathbf{F} \in \mathcal{G}_{D_{\mathbf{F}}}^3.$$

- The pair  $\mathbf{w} = (w^{(1)}, w^{(2)})$  of spline functions is contained in the glued spline space defined by  $D_{\mathbf{F}}$  if and only if the corresponding isogeometric function  $\nu$  is  $C^1$  smooth, i.e.,  $\nu \in \mathcal{V}_{\mathbf{F}}$ . Thus any  $C^1$  smooth geometrically continuous isogeometric function is simply the push forward of a glued spline function, i.e.,

$$\mathcal{V}_{\mathbf{F}} = \mathcal{G}_{D_{\mathbf{F}}} \circ \mathbf{F}^{-1}. \quad (7)$$

So far, we considered geometric gluing data  $D_{\mathbf{F}}$  defined by a given geometry mapping  $\mathbf{F}$ . Now we will start from general gluing data  $D$  and use it to define a geometry mapping. We will see, this mapping yields geometric gluing data that is essentially equivalent to  $D$  (see also [8] for the bivariate case):

**Lemma 1.** *We consider regular gluing data  $D = (\alpha_1, \alpha_2, \alpha_3, \alpha_4)$  and a regular two-patch geometry mapping  $\mathbf{F} \in \mathcal{G}_D^3$ . The geometric gluing data  $D_{\mathbf{F}}$  defined by  $\mathbf{F}$  satisfies*

$$D_{\mathbf{F}} = \phi D \quad (8)$$

with the non-zero factor

$$\phi(\xi_1, \xi_2) = \frac{J_{44}}{\alpha_4(\xi_1, \xi_2)}.$$

*Proof.* The fact that  $\mathbf{F} \in \mathcal{G}_D^3$  implies

$$\partial_3 \mathbf{F}^{(2)}|_{\xi_3=0} = \left( \frac{\alpha_1}{\alpha_4} \partial_1 \mathbf{F}^{(1)} - \frac{\alpha_2}{\alpha_4} \partial_2 \mathbf{F}^{(1)} + \frac{\alpha_3}{\alpha_4} \partial_3 \mathbf{F}^{(1)} \right)|_{\xi_3=0},$$

since the regularity of the gluing data ensures  $\alpha_4 \neq 0$ . Substituting the fourth column of the matrix in (5) by the right-hand side of this equation gives minors

$$J_{41} = \frac{\alpha_1}{\alpha_4} J_{44}, \quad J_{42} = \frac{\alpha_2}{\alpha_4} J_{44}, \quad J_{43} = \frac{\alpha_3}{\alpha_4} J_{44}. \quad (9)$$

The regularity of the geometry mapping implies  $J_{44} \neq 0$  at all points, hence combining (9) with the definition (6) of the geometric gluing data  $D_{\mathbf{F}}$  completes the proof.  $\square$

As an immediate consequence of (8) we obtain that the two glued spline spaces are identical,

$$\mathcal{G}_{D_{\mathbf{F}}} = \mathcal{G}_D \quad (10)$$

since the glued spline spaces defined by  $D$  and  $\psi D$  are identical for any non-zero factor  $\psi$ .

Finally we use these results to re-derive the recent result of Groisser and Peters [14] in our particular situation ( $C^1$  smooth isogeometric trivariate functions):

**Theorem 2.** *Consider regular gluing data  $D$  and regular geometry mapping  $\mathbf{F} \in \mathcal{G}_D^3$ . Any  $C^1$ -smooth geometrically continuous isogeometric function is the push-forward of a glued spline function,*

$$\mathcal{V}_{\mathbf{F}} = \mathcal{G}_D \circ \mathbf{F}^{-1}.$$

*Proof.* This can be seen by combining (7) and (10).  $\square$

The fundamental result of Groisser and Peters [14] deals with  $G^k$ -smoothness of  $m$ -variate geometry mappings into  $d$ -dimensional space and considers functions with values in  $\mathbb{R}^N$ . According to their result,  $G^k$  constructions always yield  $C^k$ -smooth isogeometric functions. When applying it to our specific case ( $k = 1, m = 3, d = 3$  and  $N = 1$ ), it allows to conclude that  $\mathcal{G}_D \circ \mathbf{F}^{-1} \subseteq \mathcal{V}_{\mathbf{F}}$ . The above theorem complements this observation by establishing the equivalence of both spaces under an additional regularity assumption. We conjecture that it can be extended to the general case as well. This, however, would require more technicalities and is therefore beyond the scope of the present work.

## 4 Particular classes of gluing data

We define several types of gluing data and introduce the generic dimension of the associated glued spline spaces.

### 4.1 Types of gluing data

We analyze the dimension of the glued spline space  $\mathcal{G}_D$  — and hence also the dimension of the space of  $C^1$ -smooth geometrically continuous isogeometric functions  $\mathcal{V}_{\mathbf{F}}$  for any regular geometry mapping  $\mathbf{F} \in \mathcal{G}_D^3$  — for specific types of gluing data. In general, the dimension is very low. Even for geometric gluing data, the dimension may be as low as four. Due to the linear precision of tensor-product B-splines, the space of  $C^1$ -smooth geometrically continuous isogeometric functions always contains the four-dimensional space of linear polynomials, but it does not contain any additional function in general. However, this space is guaranteed to contain *any* polynomial of degree  $p$  if we consider geometric gluing data derived from a regular trilinear geometry mapping  $\mathbf{F} \in \mathcal{G}_D^3$ , hence its dimension is at least  $\binom{p+2}{2}$  in this situation.

In order to obtain a non-trivial glued spline space  $\mathcal{G}_D$ , we consider polynomial gluing data of relatively low degree, i.e.,

$$D = (\alpha_1, \alpha_2, \alpha_3, \alpha_4) \in \Pi^{q_1} \times \Pi^{q_2} \times \Pi^{q_3} \times \Pi^{q_4},$$

where  $\Pi^{q_i}$  denotes the space of bivariate tensor-product polynomials of bi-degree  $\mathbf{q}_i \in \mathbb{Z}_{\geq 0}^2$ . The four bi-degrees  $\mathbf{Q} = [\mathbf{q}_1, \mathbf{q}_2, \mathbf{q}_3, \mathbf{q}_4]$  thus characterize a class of gluing data. In particular we obtain the degree

$$\mathbf{Q}_3 = [(3, 2), (2, 3), (2, 2), (2, 2)] \tag{11}$$

when considering geometric gluing data which is derived from a generic trilinear geometry mapping.

We analyze the dimension of  $\mathcal{G}_D$  for gluing data whose degree does not exceed  $\mathbf{Q}_3$ . The full set of all these gluing data forms a 42-dimensional real linear space, which we will denote by  $\mathcal{D}$ . In addition to considering the full space, we will also analyze the dimension for gluing data  $D$  taken from certain subsets of  $\mathcal{D}$ . These subspaces are defined as embeddings

$$\mathcal{T}_{\text{type}} : \mathbb{R}^m \rightarrow \mathcal{D},$$

of the  $m$ -dimensional real linear space  $\mathbb{R}^m$ , for some dimension  $m \in \mathbb{Z}_{>0}$ . The embeddings are represented by rational mappings  $\mathcal{T}_{\text{type}}$ , where the lower index identifies the type of gluing

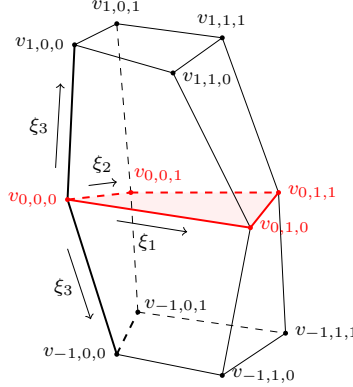


Figure 2: Two-patch geometry with two trilinear subdomains  $\Omega^{(1)}, \Omega^{(2)}$  joined at a common interface  $\Gamma$  and their defining corner points  $v_{j,k,\ell}$ .

data. Consequently, the associated subsets

$$\mathfrak{T}_{\text{type}} = \mathcal{T}_{\text{type}}(\mathbb{R}^m)$$

form algebraic varieties in  $\mathcal{D} = \mathbb{R}^{42}$ .

More precisely we consider the following embeddings:

- 1) The corner points  $v_{j,k,\ell}$  of the volumetric hexahedral patches define a two-patch trilinear geometry mapping  $\mathbf{F} = (\mathbf{F}^{(1)}, \mathbf{F}^{(2)})$ ,

$$\mathbf{F}^{(i)} = \sum_{j=0}^1 \sum_{k=0}^1 \sum_{\ell=0}^1 v_{(-1)^i j, k, \ell} \beta_j(\xi_1) \beta_k(\xi_2) \beta_\ell(\xi_3),$$

where the blending functions  $\beta_j, \beta_k, \beta_\ell$  are the linear Bernstein polynomials, see Fig. 2. We obtain geometric gluing data by evaluating the subdeterminants  $J_{4m}$  as in (5). The mapping

$$\mathcal{T}_{\text{trl}} : \mathbb{R}^{36} \rightarrow \mathcal{D}, \quad \mathbf{F} \mapsto (J_{41}, J_{42}, J_{43}, J_{44}),$$

which transforms the 36 coordinates of the 12 corner points into the associated geometric gluing data, defines the algebraic variety  $\mathfrak{T}_{\text{trl}}$  of *trilinear* geometric gluing data.

- 2) Considering again the situation of the trilinear embedding, we obtain the special case of planar interfaces<sup>1</sup> by choosing corner points  $v_{0,k,\ell} \in \mathbb{R}^2 \times \{0\}$ . The mapping

$$\mathcal{T}_{\text{pln}} : \mathbb{R}^{32} \rightarrow \mathcal{D},$$

which transforms the 32 free coordinates of the 12 corner points into the associated geometric gluing data, defines the algebraic variety  $\mathfrak{T}_{\text{pln}} \subseteq \mathfrak{T}_{\text{trl}}$  of trilinear geometric gluing data with a *planar* interface.

<sup>1</sup>Without loss of generality we choose the  $xy$  plane as the plane containing the interface.

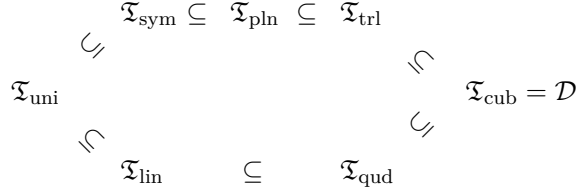


Figure 3: The relations between the algebraic varieties  $\mathfrak{T}_{\text{type}}$ , which are defined by different types of gluing data  $D$ .

- 3) Even more restrictive choices of the 12 corner points define further types of gluing data. As an example, we focus on configurations which are *symmetric* with respect to the interface plane and obtain the embedding

$$\mathcal{T}_{\text{sym}} : \mathbb{R}^{20} \rightarrow \mathcal{D},$$

defining the variety  $\mathfrak{T}_{\text{sym}} \subseteq \mathfrak{T}_{\text{pln}}$ .

- 4) In the simplest possible situation, we arrive at a two-patch domain that consists of cubes with some edge length  $\delta > 0$ . This corresponds to the classical case of *uniform*  $C^1$ -smooth splines. The associated geometric gluing data defines the embedding

$$\mathcal{T}_{\text{uni}} : \mathbb{R}^1 \rightarrow \mathcal{D},$$

which specifies the variety  $\mathfrak{T}_{\text{uni}} \subseteq \mathfrak{T}_{\text{sym}}$ .

- 5) For the sake of completeness we also include the most general case of using generic gluing data  $D$  of degree  $\mathbf{Q}_3$  as in (11). We will in the following denote such non-trilinear gluing data of degree  $\mathbf{Q}_3$  as *cubic* gluing data. By considering the 42 coefficients of these four tensor-product polynomials we find the embedding

$$\mathcal{T}_{\text{cub}} : \mathbb{R}^{42} \rightarrow \mathcal{D},$$

which defines the full set  $\mathfrak{T}_{\text{cub}} = \mathcal{D}$ .

- 6) Considering again the situation of the generic embedding, we obtain the special cases of *quadratic* and *linear* gluing data by restricting some of the coefficients of the four polynomials  $\alpha_i$ ,  $i \in \{1, 2, 3, 4\}$  to zero. In particular, we consider the degrees

$$\mathbf{Q}_2 = [(2, 1), (1, 2), (1, 1), (1, 1)] \quad \text{and} \quad \mathbf{Q}_1 = [(1, 0), (0, 1), (0, 0), (0, 0)],$$

respectively and obtain the embeddings

$$\mathcal{T}_{\text{qud}} : \mathbb{R}^{20} \rightarrow \mathcal{D} \quad \text{and} \quad \mathcal{T}_{\text{lin}} : \mathbb{R}^6 \rightarrow \mathcal{D}$$

which define the varieties  $\mathfrak{T}_{\text{lin}} \subseteq \mathfrak{T}_{\text{qud}}$ .

Figure 3 summarizes the relation between the algebraic varieties in the space  $\mathcal{D}$  which correspond to the various types of gluing data described above.

## 4.2 Generic dimension

For given gluing data  $D \in \mathcal{Q}_3$  we compute the dimension of the glued spline space  $\mathcal{G}_D$  by analyzing the equations (2). The right-hand sides of both equations are contained in the spline space  $\mathcal{P}' = \mathcal{S}_{0,k}^{p+2} \otimes \mathcal{S}_{0,k}^{p+2}$ . Thus we obtain an equivalent homogeneous linear system<sup>2</sup>

$$A_D \mathbf{b} = \mathbf{0} \tag{12}$$

for the unknowns

$$\mathbf{b} = \left( b_j^{(i)} \right)_{j=1, \dots, n, i=1, 2} \tag{13}$$

by performing collocation at the Greville points of  $\mathcal{P}'$ . The dimension of the glued spline space is determined by the rank of the coefficient matrix,

$$\dim \mathcal{G}_D = 2n - \text{rank } A_D.$$

For fixed values of  $p$  and  $k$ , the dimension defines a function on the 42-dimensional space  $\mathcal{D}$ .

In order to compute the dimension, we evaluate the rank of the matrix  $A_D$ . We pay special attention to avoid numerical errors during the computation. To do so, we use *rational* numbers throughout the process. The Greville abscissas have rational coordinates and the values of B-spline functions on them are also rational, which is why the matrix  $A_D$  is a matrix with rational elements as well. Later, in order to obtain a basis, we will also compute the kernel of the matrix  $A_D$  and analyze the structure of the solutions. More precisely we apply Gaussian elimination to transform  $A_D$  to Reduced Row Echelon Form (RREF).

Recall that the rank of the coefficient matrix satisfies

$$\text{rank } A_D = \min_{r \in \mathbb{N}} \{ r : \text{all } (r+1) \times (r+1) \text{ minors of } A_D \text{ vanish} \}.$$

Consequently, when adopting the notion of *degeneracy loci* from [11],

$$\mathfrak{L}_r = \{ D \in \mathcal{D} : \text{rank } A_D \leq r \},$$

it is obvious that these loci form a nested sequence of algebraic varieties,

$$\{(0, 0, 0, 0)\} = \mathfrak{L}_0 \subseteq \dots \subseteq \mathfrak{L}_r \subseteq \mathfrak{L}_{r+1} \subseteq \dots \subseteq \mathfrak{L}_{2n} = \mathcal{D}.$$

The dimension  $\mathcal{G}_D$  is at least  $2n - r$  if the degeneracy locus  $\mathfrak{L}_r$  contains the gluing data  $D \in \mathcal{D}$ .

In order to capture the dimension of the glued spline space for an entire class of gluing data — which is defined by one of the types introduced in the previous section — we define the *generic* dimension  $\delta_{\text{type}}$  as

$$\delta_{\text{type}} = 2n - \min_r \{ r : \mathfrak{T}_{\text{type}} \subseteq \mathfrak{L}_r \}.$$

This notion is justified by the following observation:

**Theorem 3.** *For randomly chosen gluing data  $D \in \mathfrak{T}_{\text{type}}$ , where *type* is one of the types introduced in Section 4, the dimension of the glued spline space satisfies*

$$\dim \mathcal{G}_D = \delta_{\text{type}}$$

*with probability 1.*

---

<sup>2</sup>In practice, it suffices to analyze the smaller system obtained by identifying the degrees of freedom along the common interface and restricting the system to the three layers of coefficients around it.

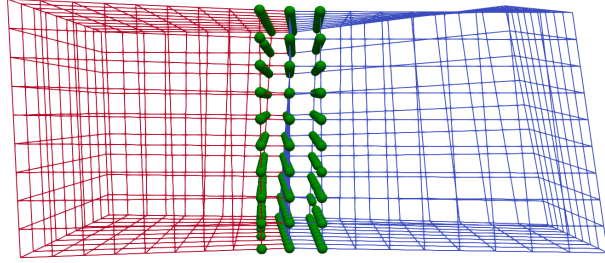


Figure 4: Coefficients used by the interface functions (green bullets). The figure shows the control cages of both patches (red and blue).

*Proof.* Recall that the degeneracy loci can be characterized by vanishing minors of the coefficient matrix  $A_D$ . More precisely, the degeneracy loci satisfy

$$\mathfrak{L}_r = \{D : s_r(D) = 0\},$$

where  $s_r(D)$  is the vector whose elements are all the  $(r+1) \times (r+1)$ -minors of  $A_D$ . Consequently, the inclusion  $\mathfrak{T}_{\text{type}} \subseteq \mathfrak{L}_r$  can equivalently be characterized by

$$s_r \circ \mathcal{T}_{\text{type}} = 0 \quad \text{on } \mathbb{R}^m,$$

where  $m$  is the dimension of the preimage space of the embeddings  $\mathcal{T}_{\text{type}}$ .

We consider the randomly chosen gluing data  $D \in \mathfrak{T}_{\text{type}}$ . For any  $r$ , the equations  $s_r \circ \mathcal{T}_{\text{type}} = 0$  define an algebraic variety, which is either the entire space  $\mathbb{R}^m$ , or it is a lower-dimensional subvariety thereof. The latter case occurs if and only if  $r < 2n - \delta_{\text{type}}$ , due to the definition of the generic dimension. Consequently, for any randomly generated point  $x \in \mathbb{R}^m$ ,

$$P\left((s_r \circ \mathcal{T}_{\text{type}})(x) = 0\right) = \begin{cases} 1, & \text{if } \mathfrak{T}_{\text{type}} \subseteq \mathfrak{L}_r \\ 0, & \text{otherwise,} \end{cases}$$

since lower dimensional subvarieties of  $\mathbb{R}^m$  have zero volume. Thus

$$P\left(\min_r \{(s_r \circ \mathcal{T}_{\text{type}})(x) = 0\} = \min_r (\mathfrak{T}_{\text{type}} \subseteq \mathfrak{L}_r)\right) = 1$$

which implies

$$P(\dim \mathcal{G}_D = \delta_{\text{type}}) = 1$$

and this completes the proof.  $\square$

## 5 Dimension of the glued spline space

The different types of gluing data  $\mathcal{T}_{\text{type}} \subseteq D$  yield different dimensions  $\delta_{\text{type}}$ . We adopt the strategy introduced in [25, Theorem 4] and extend it to the trivariate case. More precisely, we split the glued spline space into a direct sum of spaces of *inner* functions and *interface* functions. The nonzero spline coefficients of the latter ones are located in the three layers adjacent to the interface, while the inner functions use only the remaining coefficients, see Fig. 4.

$k$	$p=2$	$p=3$	$p=4$	$p=5$	$p=6$	$p=7$	$p=8$
0	18+2	64+12	150+26	288+44	490+66	768+92	1134+122
1	64+2	288+12	768+37	1600+85	2880+153	4704+237	7168+337
2	150+2	768+12	2178+50	4704+136	8670+274	14400+448	22218+658
3	288+2	1600+12	4704+65	10368+197	19360+429	32448+725	50400+1085
4	490+2	2880+12	8670+82	19360+268	36450+618	61440+1068	95830+1618

Table 1: Dimensions  $\delta^0 + \delta_{\text{cub}}^\Gamma$  of glued spline spaces for cubic gluing data.

The dimension of the space of inner functions

$$\delta^0 = 2(p+1+k(p-1))^2(p-1+k(p-1))$$

does not depend on the gluing data, since their values and first derivatives vanish along the interface. We analyze the dimension of the interface functions by studying randomly generated instances. Each instance provides a lower bound on the dimension. However, since we use random instances, the sum of both dimensions

$$\delta_{\text{type}} = \delta^0 + \delta_{\text{type}}^\Gamma$$

is equal to the generic dimension with probability 1 due to the Theorem 3.

We now proceed by discussing  $\delta_{\text{type}}^\Gamma$  for the various types of gluing data individually.

**Type ‘cub’** First we consider general cubic gluing data. Table 1 presents the dimensions  $\delta_{\text{cub}}$  for different degrees  $(p, p, p)$  and numbers  $k$  of inner knots. The dimension of the space  $\mathcal{G}_D$  is shown as the sum of the dimensions of the spaces of inner and the interface functions. While the dimension of the inner functions grows with  $k$  for any degree  $p$ , the number of linearly independent interface functions remains constant for  $p = 3$ .

We use interpolation to obtain a closed formula for the dimension of the interface functions. One expects to obtain a closed polynomial expression for sufficiently large degrees  $p$ , but not necessarily for all degrees. In the case of cubic gluing data, we did not obtain a closed formula when considering degrees  $p \leq 4$ . For  $p > 4$ , we conjecture that the dimension satisfies

$$\delta_{\text{cub}}^\Gamma = -6 - 14k + 5k^2 - 10k(1+k)p + 2(k+1)^2 p^2$$

for generic cubic gluing data.

**Type ‘trl’** Table 2 presents the dimensions  $\delta_{\text{trl}}$  for the case of trilinear geometric gluing data. The dimensions are always larger than in the cubic case. This is significantly different from the results in [8] for the bivariate case, where it was shown that the dimension does not change when generalizing bilinear parameterizations to *analysis-suitable*  $G^1$  parameterizations, see Remark 4 below for more details.

Again we use interpolation to obtain a closed formula for the dimension of the interface functions. For  $p > 2$ , we conjecture that the dimension satisfies

$$\delta_{\text{trl}}^\Gamma = 2 + 2k + 13k^2 - 10k(1+k)p + 2(k+1)^2 p^2.$$

$k$	$p=2$	$p=3$	$p=4$	$p=5$	$p=6$
0	18+10	64+20	150+34	288+52	490+74
1	64+10	288+29	768+65	1600+117	2880+185
2	150+10	768+40	2178+106	4704+208	8670+346
3	288+10	1600+53	4704+157	10368+325	19360+557
4	490+10	2880+68	8670+218	19360+468	36450+818

Table 2: Dimensions  $\delta^0 + \delta_{\text{trl}}^\Gamma$  of glued spline spaces for trilinear geometric gluing data.

$k$	$p=2$	$p=3$	$p=4$	$p=5$	$p=6$
0	18+15	64+27	150+43	288+63	490+87
1	64+22	288+49	768+93	1600+153	2880+229
2	150+31	768+79	2178+163	4704+283	8670+439
3	288+42	1600+117	4704+253	10368+453	19360+717
4	490+55	2880+163	8670+363	19360+663	36450+1063

Table 3: Dimensions  $\delta^0 + \delta_{\text{sym}}^\Gamma$  of glued spline spaces for trilinear gluing data corresponding to two symmetric trilinear subdomains.

$k$	$p=2$	$p=3$	$p=4$	$p=5$	$p=6$
0	18+18	64+32	150+50	288+72	490+98
1	64+32	288+72	768+128	1600+200	2880+288
2	150+50	768+128	2178+242	4704+392	8670+578
3	288+72	1600+200	4704+392	10368+648	19360+968
4	490+98	2880+288	8670+578	19360+968	36450+1458

Table 4: Dimensions  $\delta^0 + \delta_{\text{uni}}^\Gamma$  of glued spline spaces for gluing data  $\mathcal{T}_{\text{uni}}$ .

**Type ‘pln’** This class of gluing data is derived from trilinear parametrizations with planar interfaces. We obtain exactly the same results as in the previous case (Table 2), hence  $\delta_{\text{pln}} = \delta_{\text{trl}}$ .

**Type ‘sym’** An even more restricted class of gluing data is derived from symmetric trilinear parametrizations. Table 3 lists the dimensions  $\delta_{\text{sym}}$  for this situation as the sum of  $\delta^0 + \delta_{\text{sym}}^\Gamma$ . The dimensions are always larger than in the previous three cases.

Again we use interpolation to obtain a closed formula for  $\delta_{\text{sym}}^\Gamma$ . For  $p > 2$ , we conjecture that the dimension satisfies

$$\delta_{\text{sym}}^\Gamma = 3 + 10k^2 + 2(1 - 3k - 4k^2)p + 2(k + 1)^2 p^2.$$

**Type ‘uni’** Table 4 presents the dimensions  $\delta_{\text{uni}}$  for the case of gluing data that corresponds to two cubes with a shared face. The obtained dimensions are always larger than for the other cases.

We arrive at the closed formula for the dimension of the interface functions,

$$\delta_{\text{uni}}^\Gamma = 2(1 - k)^2 + 4(1 - k^2)p + 2(k + 1)^2 p^2,$$

which is equal to the dimension of the interface functions among the trivariate tensor-product splines on the two cubes.

$k$	$p=2$	$p=3$	$p=4$	$p=5$	$p=6$	$p=7$
0	18+11	64+23	150+39	288+59	490+83	768+111
1	64+11	288+34	768+77	1600+137	2880+213	4704+305
2	150+11	768+47	2178+127	4704+247	8670+403	14400+595
3	288+11	1600+62	4704+189	10368+389	19360+653	32448+981
4	490+11	2880+79	8670+263	19360+563	36450+963	61440+1463

Table 5: Dimensions  $\delta^0 + \delta_{\text{qud}}^\Gamma$  of glued spline spaces for gluing data of degree  $\mathbf{Q}_2$

$k$	$p=2$	$p=3$	$p=4$	$p=5$	$p=6$
0	18+18	64+32	150+50	288+72	490+98
1	64+25	288+61	768+113	1600+181	2880+265
2	150+34	768+100	2178+202	4704+340	8670+514
3	288+45	1600+149	4704+317	10368+549	19360+845
4	490+58	2880+208	8670+458	19360+808	36450+1258

Table 6: Dimensions  $\delta^0 + \delta_{\text{lin}}^\Gamma$  of glued spline spaces for gluing data of degree  $\mathbf{Q}_1$

**Types ‘qud’ and ‘lin’** Table 5 presents the dimensions  $\delta_{\text{qud}}$  for gluing data  $D$  of degree  $\mathbf{Q}_2$ . The obtained dimensions are always larger than in case of cubic gluing data. Again we use interpolation to obtain a closed formula for the dimension of the interface functions. For  $p > 3$ , we conjecture that the dimension satisfies

$$\delta_{\text{qud}}^\Gamma = -1 - 8k + 6k^2 + 2(1 - 3k - 4k^2)p + 2(k + 1)^2 p^2.$$

Table 6 presents the dimensions  $\delta_{\text{lin}}$  for gluing data  $D$  of degree  $\mathbf{Q}_1$ . The obtained dimensions are always larger than in case of quadratic gluing data. For  $k = 0$  and any choice of  $p$  we obtain the same dimension  $\delta_{\text{lin}}$  as for gluing data of type ‘uni’.

For  $p > 2$ , we conjecture that the dimension satisfies

$$\delta_{\text{lin}}^\Gamma = 2 - 6k + 5k^2 + 2(2 - k - 3k^2)p + 2(k + 1)^2 p^2.$$

*Remark 4.* For the *trivariate* isogeometric functions considered in this paper, the spaces defined by cubic gluing data (more precisely, by gluing data of degree  $\mathbf{Q}_3$ , see (11)) and by trilinear geometric gluing data have different dimensions. This is due to the fact that the algebraic varieties defined by the embeddings  $\mathcal{T}_{\text{cub}}$  and  $\mathcal{T}_{\text{trl}}$  are different. Indeed, the second one is a proper subvariety of the first one. This is a fundamental difference to the bivariate case. In that case, we have to consider only three blending functions, which depend solely on one variable. The two classes of gluing data, which correspond to the types cub and trl, are data of degree  $(2, 1, 1)$  [8] and geometric data generated by bilinear geometry mappings [25], respectively. A short computation confirms that the two associated subvarieties are identical. Indeed, one can prove that the subset associated with the bilinear gluing data is dense in the algebraic variety generated by the data of degree  $(2, 1, 1)$ . Consequently, the generic dimensions of the corresponding glued spline spaces are identical. In particular, this also applies to the particular class of analysis-suitable gluing data, which is situated between the two classes, see [21].

36	48	60	72	84	96	0	6	12	18	24	30	37	49	61	73	85	97
•	•	•	•	•	•	•	•	•	•	•	•	•	•	•	•	•	•
38	50	62	74	86	98	1	7	13	19	25	31	39	51	63	75	87	99
•	•	•	•	•	•	•	•	•	•	•	•	•	•	•	•	•	•
40	52	64	76	88	100	2	8	14	20	26	32	41	53	65	77	89	101
•	•	•	•	•	•	•	•	•	•	•	•	•	•	•	•	•	•
42	54	66	78	90	102	3	9	15	21	27	33	43	55	67	79	91	103
•	•	•	•	•	•	•	•	•	•	•	•	•	•	•	•	•	•
44	56	68	80	92	104	4	10	16	22	28	34	45	57	69	81	93	105
•	•	•	•	•	•	•	•	•	•	•	•	•	•	•	•	•	•
46	58	70	82	94	106	5	11	17	23	29	35	47	59	71	83	95	107
•	•	•	•	•	•	•	•	•	•	•	•	•	•	•	•	•	•

Figure 5: Numbering of the three layers of coefficients of interface basis functions for  $p = 3$  and  $k = 1$ . From left to right: coefficients above, on and below the interface.

## 6 Basis functions

In order to obtain glued spline spaces (and consequently spaces of  $C^1$ -smooth geometrically continuous isogeometric functions) on two-patch domains that are useful for applications, we investigate two additional questions:

1. Can we find a system of locally supported<sup>3</sup> basis functions spanning the space?
2. Do these functions have good approximation properties?

We will focus mainly on the first question and give partial answers to the second one in the next section. Basis functions for a specific case will be presented in Section 6.2.

### 6.1 Existence of a locally supported basis

In order to simplify the presentation and to eliminate the influence of boundary effects, we restrict ourselves to spaces with homogeneous  $C^1$  boundary conditions. This does not limit the applicability of the results to isogeometric analysis since one may always transform inhomogeneous problems into homogeneous ones. The glued spline space which is obtained by enforcing these conditions will be denoted by  $\mathcal{G}_{D,0}$ . Consequently, we may discard two layers of boundary coefficients from the equations (2) and the equivalent linear system (12).

We focus on the computation of interface basis functions  $\delta_{\text{type}}^{\Gamma}$  and their structure for different types of generic gluing data and various degrees. In order to find locally supported basis functions, we order the coefficients  $\mathbf{b}$  (see (13)) according to their location. Figure 5 shows this ordering for a particular case.

After reordering the columns of  $A_D$  according to this numbering (and discarding boundary coefficients), we compute the coefficients of the basis functions using the RREF of the matrix. In most cases we were able to identify patterns for the kernel of the matrix, which correspond to locally supported interface basis functions. More precisely, we obtained four classes of functions, visualized by different symbols in Table 7:

- × No locally supported interface basis functions were found,  $\dim \mathcal{G}_{D,0} = 0$ . In these cases, the dimension of the full space of glued spline functions does not depend on  $k$ .
- (×) Locally supported basis functions were found but they take only zero values on the interface. This implies locking and hence a loss of approximation power.

<sup>3</sup>More precisely, we wish to have basis functions with a bounded number of non-zero-coefficients, where the bound is independent of the number of inner knots  $k$ .

$p$	Trilinear gluing data	Cubic gluing data	Quadratic gluing data	Linear gluing data
2	×	×	×	(×)
3	✓	×	(×)	(×)
4	✓	(×)	(×)	✓
5	✓	(×)	(✓)	✓

Table 7: This table shows the different types of bases occurring for the specific types of gluing data. × indicates that  $\dim \mathcal{G}_{D,0} = 0$  and (×) that only basis functions with zero support on the shared face were obtained, hence leading to locking. Entries with ✓ refer to local bases with desired properties at the interface. (✓) signals that a basis was constructed not fulfilling all requirements for local support.

✓ We found a local basis of the space  $\mathcal{G}_{D,0}$  and there are basis functions with non-zero coefficients on the interface.

(✓) We found a basis of the space  $\mathcal{G}_{D,0}$  but not all basis functions are local.

Only global basis functions were found for almost all types of gluing data if  $p = 2$ , and for cubic gluing data if  $p = 3$ . This matches the corresponding dimensions results of Section 5, which showed that the dimension of the interface functions does not increase with the number  $k$  of inner knots. Among the other cases, the most promising ones are trilinear and linear gluing data of degree  $p \geq 3$  and  $p \geq 4$ , respectively. The case of quintic splines for quadratic gluing data is still open, since applying a re-ordering of the coefficients might still lead to a locally supported basis.

## 6.2 Basis functions for trilinear geometric gluing data

In this section we discuss the obtained interface functions in case of trilinear geometric gluing data  $\mathcal{T}_{\text{trl}}$  and  $C^1$  boundary conditions in further detail, focusing on degrees  $p = 3, 4$ . Similar results can be obtained for higher degrees. Independently of the spline degree  $p > 2$ , we obtain a local basis containing functions taking non-zero values on the interface, provided that there are sufficiently many inner knots. For applications it is important to understand the structure of the basis functions, i.e., their coefficient patterns.

For degree  $p = 3$ , the basis can be generated by using functions of only one type. The coefficient pattern, which involves  $6 \times 6 \times 3$  coefficients, is shown in Fig. 6 (top). More precisely, the three pictures represent the three layers of relevant spline coefficients (from left to right: above, on, and below the interface), specifying the signs of these coefficients. The basis is formed by  $(k - 2)^2$  functions of this type, with coefficient patterns obtained by performing index shifts by multiples of  $p - 1 = 2$  (horizontally and/or vertically).

The values of these functions are visualized by an isosurface (middle row, left) and by the level curves in a plane that intersects the interface transversally (right). These level curves are connected smoothly across the interface, thereby confirming the  $C^1$  smoothness of the basis. Additionally we provide reflection lines of a particular level set (bottom).

This approach can be generalized to basis functions of degree  $p = 4$ . In this case we distinguish between six types of basis functions, depending on the number of non-zero coefficients. The coefficients form seven different patterns, one for each of the types 1 and 3-6, and two for type 2, see Figure 7. Figure 8 visualizes these functions. The global  $C^1$ -smoothness is confirmed by the smoothness of the level curves (right column).

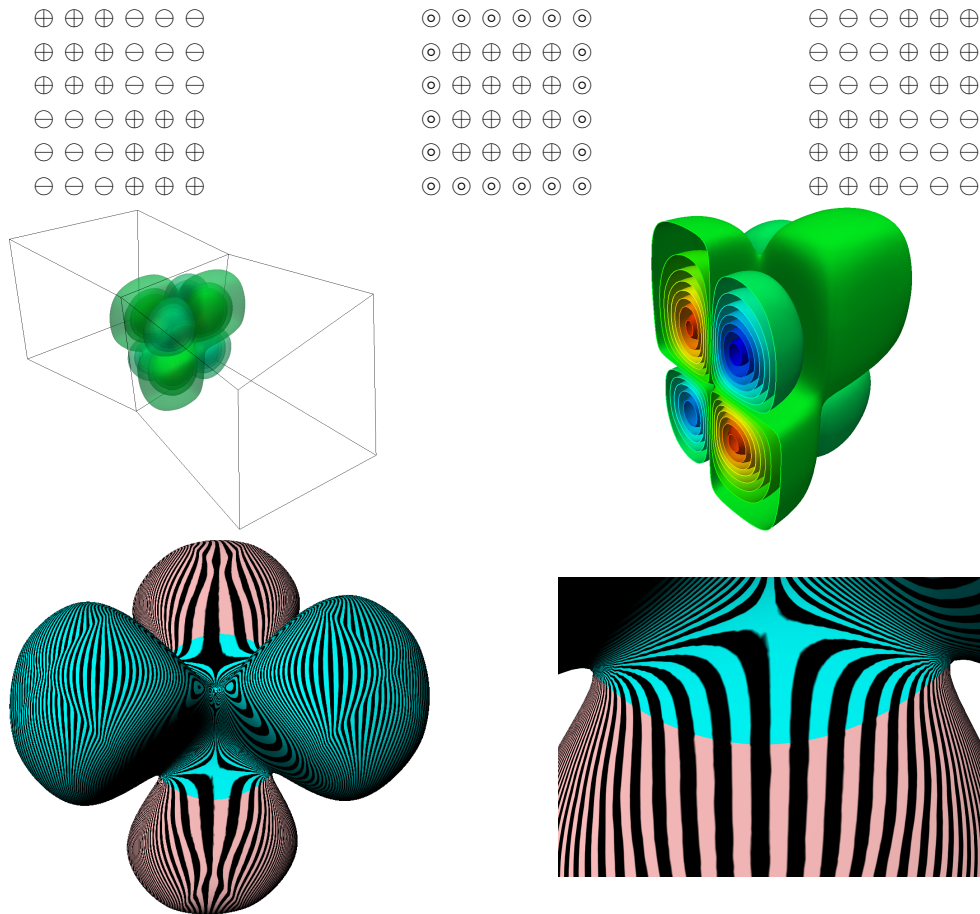


Figure 6: Coefficient pattern (top), function values (middle, visualized by isosurfaces (left) and a level curves in a plane (right)) and reflection lines of a particular level set (bottom) of the single type of basis functions obtained for  $p = 3$ .

Different instances of the basis functions are obtained when using coefficient patterns obtained by performing index shifts by multiples of  $p - 1 = 3$  (horizontally and/or vertically). Not all the functions obtained in this way are present in the basis of the glued spline space:

- Only the  $2k - 1$  translates obtained by applying index shifts to either one of the two indices are considered for the Type 1 pattern.
- Only the  $k - 1$  translates obtained by applying horizontal index shifts are considered for the Type 2.1 pattern.
- For all other types, we use all possible translates, resulting in  $k(k - 1)$  functions of Type 2.2 and  $(k - 1)^2$  functions for each of the remaining types.

Summing up, the size of the basis amounts to  $5k^2 - 6k + 2$ , assuming that  $k$  is non-zero.

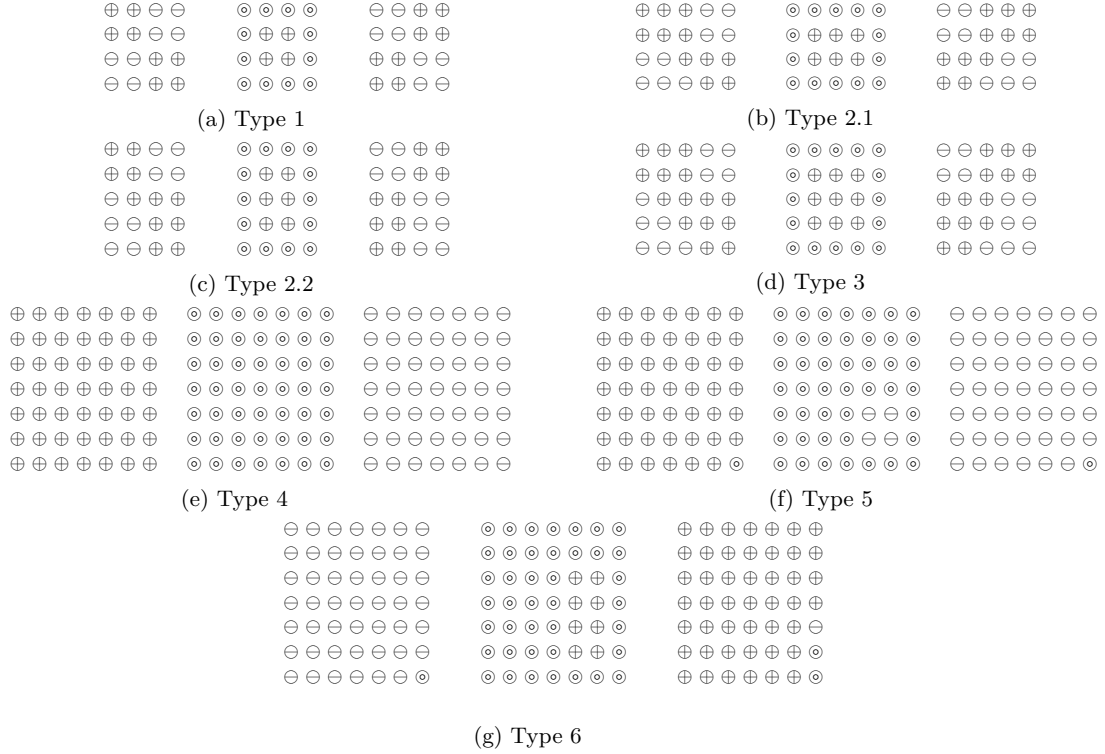


Figure 7: Coefficient patterns of basis functions obtained for  $p = 4$ .

## 7 Conclusions

We analyzed the spaces of  $C^1$ -smooth geometrically continuous isogeometric functions on hexahedral two-patch domains. We introduced the notation of gluing data and used it to define glued spline functions on two-patch domains. We were able to characterize  $C^1$ -smooth geometrically continuous isogeometric functions as push-forwards of glued spline functions.

In addition to these theoretical results, we studied several classes of gluing data in more detail. More precisely, we identified several interesting types of trilinear geometric gluing data, and we considered the generic case of degree  $Q_3$  as well as lower degree cases.

We analyzed the generic dimension of the glued spline space for these classes of gluing data and showed how to construct locally supported basis functions. These functions, however, do not exist for all combinations of gluing data and degrees. Even if they exist, they may all take zero values on the interface, thereby indicating  $C^1$ -locking, cf. [8]. According to our results, the class of trilinear geometric gluing data is particularly promising for applications in isogeometric analysis since it leads to locally supported basis functions without locking for moderate degrees of the spline functions.

Our current work is devoted to the detailed investigation of the approximation power of the resulting spaces of  $C^1$ -smooth geometrically continuous isogeometric functions, and to applications in isogeometric simulations. In the bivariate case, it was shown that glued spline spaces defined by bilinear geometric gluing data possess optimal approximation properties. Moreover, this was found to be true for the class of analysis-suitable  $G^1$ -parameterizations

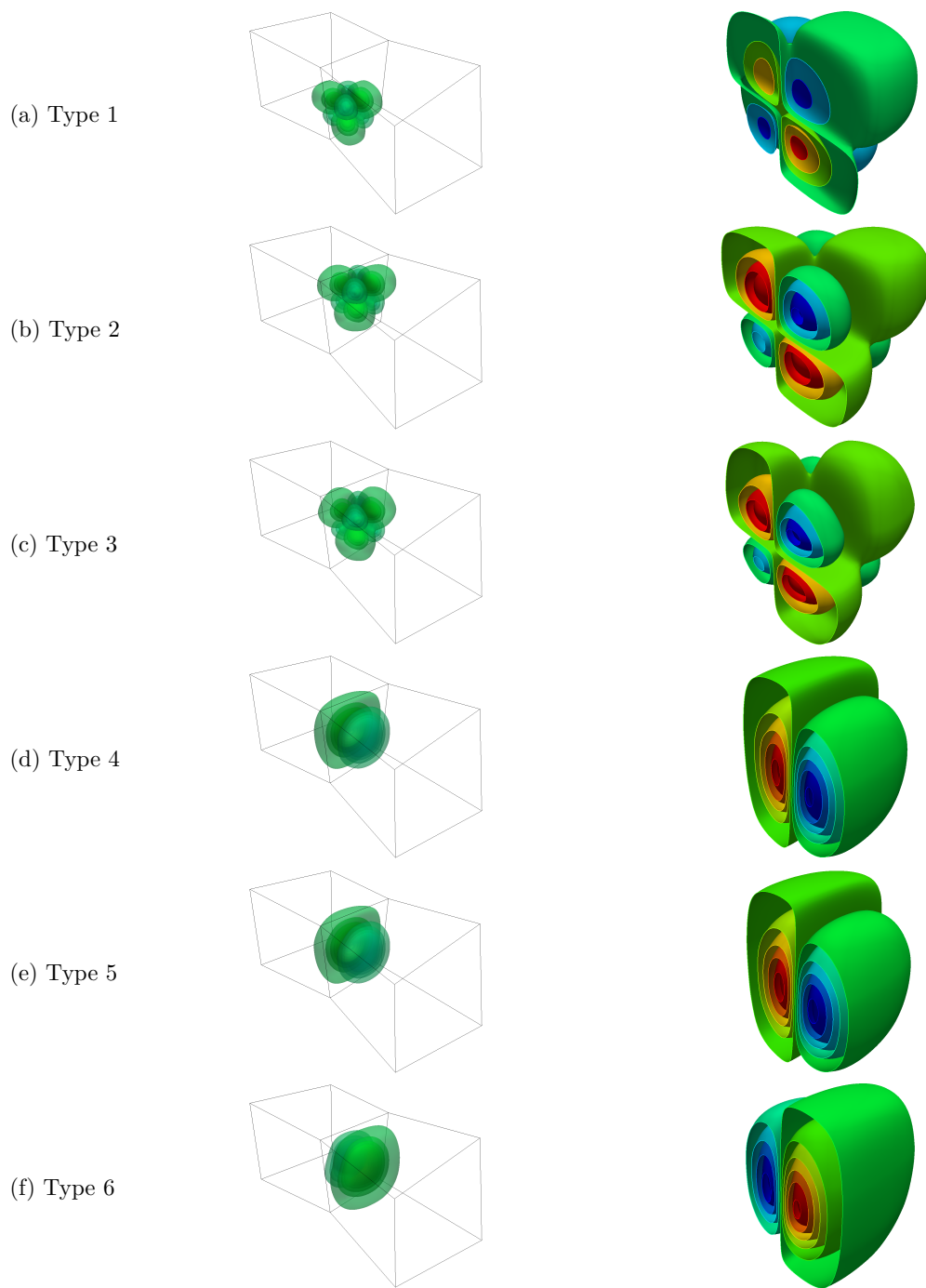


Figure 8: Isosurfaces (left column) and level curves in a plane that intersects the interface transversally (right column) visualizing the values of the six different types of basis functions obtained for  $p = 4$ .

[8]. The generalization of these results to the trivariate case is of vital interest.

Finally, the class of two-patch domains possesses rather limited geometric modeling ca-

pabilities, and hence the generalization to the full multi-patch case is a potential topic for future research, similar to the results presented in [19] for the bivariate case.

**Acknowledgment** Supported by the Austrian Science Fund (FWF) through NFN S117 “Geometry + Simulation”.

## References

- [1] A. Apostolatos, R. Schmidt, R. Wüchner, and K.-U. Bletzinger. A Nitsche-type formulation and comparison of the most common domain decomposition methods in isogeometric analysis. *International Journal for Numerical Methods in Engineering*, 97(7):473–504, 2014.
- [2] L. Beirão Da Veiga, A. Buffa, C. Lovadina, M. Martinelli, and G. Sangalli. An isogeometric method for the Reissner-mindlin plate bending problem. *Computer Methods in Applied Mechanics and Engineering*, 209:45–53, 2012.
- [3] L. Beirão Da Veiga, A. Buffa, G. Sangalli, and R. Vázquez. Mathematical analysis of variational isogeometric methods. *Acta Numerica*, 23:157–287, 2014.
- [4] D. J. Benson, Y. Bazilevs, M.-C. Hsu, and T. J. Hughes. A large deformation, rotation-free, isogeometric shell. *Computer Methods in Applied Mechanics and Engineering*, 200(13):1367–1378, 2011.
- [5] M. Bercovier and T. Matskewich. *Smooth Bézier surfaces over unstructures quadrilateral meshes*. Springer, 2017.
- [6] E. Brivadis, A. Buffa, B. Wohlmuth, and L. Wunderlich. Isogeometric mortar methods. *Computer Methods in Applied Mechanics and Engineering*, 284:292–319, 2015.
- [7] F. Buchegger, B. Jüttler, and A. Mantzaflaris. Adaptively refined multi-patch B-splines with enhanced smoothness. *Applied Mathematics and Computation*, 272:159–172, 2016.
- [8] A. Collin, G. Sangalli, and T. Takacs. Analysis-suitable  $G^1$  multi-patch parametrizations for  $C^1$  isogeometric spaces. *Computer Aided Geometric Design*, pages 93–113, 2016.
- [9] J. A. Cottrell, T. J. R. Hughes, and Y. Bazilevs. *Isogeometric analysis: toward integration of CAD and FEA*. John Wiley & Sons, 2009.
- [10] L. Dedè, M. J. Borden, and T. J. Hughes. Isogeometric analysis for topology optimization with a phase field model. *Archives of Computational Methods in Engineering*, 19:427–465, 2012.
- [11] J. A. Geertsen. Degeneracy loci of vector bundle maps and ampleness. *Mathematica Scandinavica*, pages 13–34, 2002.
- [12] H. Gómez, V. M. Calo, Y. Bazilevs, and T. J. Hughes. Isogeometric analysis of the Cahn–Hilliard phase-field model. *Computer methods in applied mechanics and engineering*, 197(49):4333–4352, 2008.

- [13] H. Gomez, T. J. Hughes, X. Nogueira, and V. M. Calo. Isogeometric analysis of the isothermal Navier–Stokes–Korteweg equations. *Computer Methods in Applied Mechanics and Engineering*, 199(25):1828–1840, 2010.
- [14] D. Groisser and J. Peters. Matched  $G^k$ -constructions always yield  $C^k$ -continuous isogeometric elements. *Computer Aided Geometric Design*, 34:67–72, 2015.
- [15] Y. Guo and M. Ruess. Nitsche’s method for a coupling of isogeometric thin shells and blended shell structures. *Computer Methods in Applied Mechanics and Engineering*, 284:881–905, 2015.
- [16] C. Hofer and U. Langer. Dual-primal isogeometric tearing and interconnecting solvers for multipatch dG-IgA equations. *Computer Methods in Applied Mechanics and Engineering*, 316:2–21, 2017.
- [17] J. Hoschek and D. Lasser. *Fundamentals of computer aided geometric design*. AK Peters, Ltd., 1993.
- [18] T. J. R. Hughes, J. A. Cottrell, and Y. Bazilevs. Isogeometric analysis: CAD, finite elements, NURBS, exact geometry and mesh refinement. *Comput. Methods Appl. Mech. Engrg.*, 194(39-41):4135–4195, 2005.
- [19] M. Kapl, F. Buchegger, M. Bercovier, and B. Jüttler. Isogeometric analysis with geometrically continuous functions on planar multi-patch geometries. *Computer Methods in Applied Mechanics and Engineering*, 2016.
- [20] M. Kapl, G. Sangalli, and T. Takacs. Construction of analysis-suitable  $G^1$  planar multi-patch parameterizations. *arXiv preprint arXiv:1706.03264*, 2017.
- [21] M. Kapl, G. Sangalli, and T. Takacs. Dimension and basis construction for analysis-suitable  $G^1$  two-patch parameterizations. *Computer Aided Geometric Design*, 52:75–89, 2017.
- [22] M. Kapl and V. Vitrih. Dimension and basis construction for  $C^2$ -smooth isogeometric spline spaces over bilinear-like  $G^2$  two-patch parameterizations. *arXiv preprint arXiv:1707.03145*, 2017.
- [23] M. Kapl and V. Vitrih. Space of  $C^2$ -smooth geometrically continuous isogeometric functions on planar multi-patch geometries: Dimension and numerical experiments. *Computers & Mathematics with Applications*, 73(10):2319–2338, 2017.
- [24] M. Kapl and V. Vitrih. Space of  $C^2$ -smooth geometrically continuous isogeometric functions on two-patch geometries. *Computers & Mathematics with Applications*, 73(1):37–59, 2017.
- [25] M. Kapl, V. Vitrih, B. Jüttler, and K. Birner. Isogeometric analysis with geometrically continuous functions on two-patch geometries. *Computers & Mathematics with Applications*, 70(7):1518–1538, 2015.
- [26] J. Kiendl, Y. Bazilevs, M.-C. Hsu, R. Wüchner, and K.-U. Bletzinger. The bending strip method for isogeometric analysis of Kirchhoff-Love shell structures comprised of multiple

- patches. *Computer Methods in Applied Mechanics and Engineering*, 199(35):2403–2416, 2010.
- [27] U. Langer, A. Mantzaflaris, S. E. Moore, and I. Touloupoulos. Multipatch discontinuous galerkin isogeometric analysis. In *Isogeometric Analysis and Applications 2014*, pages 1–32. Springer, 2015.
- [28] B. Mourrain, R. Vidunas, and N. Villamizar. Dimension and bases for geometrically continuous splines on surfaces of arbitrary topology. *Computer Aided Geometric Design*, 45:108–133, 2016.
- [29] T. Nguyen, K. Karčiauskas, and J. Peters.  $C^1$  finite elements on non-tensor-product 2D and 3D manifolds. *Applied mathematics and computation*, 272:148–158, 2016.
- [30] V. P. Nguyen, P. Kerfriden, M. Brino, S. P. Bordas, and E. Bonisoli. Nitsche’s method for two and three dimensional nurbs patch coupling. *Computational Mechanics*, 53(6):1163–1182, 2014.
- [31] J. Peters. Geometric continuity. In *Handbook of computer aided geometric design*, pages 193–227. North-Holland, Amsterdam, 2002.
- [32] M. A. Scott, D. C. Thomas, and E. J. Evans. Isogeometric spline forests. *Computer Methods in Applied Mechanics and Engineering*, 269:222–264, 2014.